Multiple Points-In-Time Estimation of Peak Wind Effects on Structures

DongHun Yeo, M.ASCE[1]

Abstract: One of the problems encountered in the estimation of wind effects on high-rise structures is the development of combinations of wind-induced translational responses in possible conjunction with rotational responses and/or of forces and moments that contribute to the wind-induced demand at various cross sections of individual structural members. In current wind engineering practice such combinations are developed in large part intuitively because phase information on the effects being combined is not readily available from frequency domain analyses. In contrast, full time series analyses can produce estimates of combined wind effects because they preserve phase information; however, such analyses can be overly time-consuming. In current wind engineering practice it is common to use the empirical point-in-time (PIT) procedure for the estimation of peaks of combined stationary stochastic processes. The procedure is applied to pairs of such processes, and consists of adding an estimate of the peak value of one of the processes to the estimated value of the second process at the time of the occurrence of that peak. Even if the full time histories of the two stochastic processes are used, errors inherent in PIT can be in some cases as high as 20% on the unconservative side. The purpose of this paper is to present the empirical multiple points-in-time (MPIT) procedure, which improves significantly upon the PIT approach. The MPIT procedure is illustrated by an application to a 60-story reinforced concrete structure. Results show that the MPIT approach produces remarkably accurate estimates of the peak combined wind effects by using a limited number of peaks from the time histories of the individual wind effects being combined. Those estimates are obtained far more economically in terms of computational time than conventional time domain estimates that use full time histories. **DOI: 10.1061/(ASCE)ST.1943-541X.0000649.** *© 2013 American Society of Civil Engineers.*

CE Database subject headings: Wind loads; Structural response; High-rise buildings; Concrete structures; Reinforced concrete.

Author keywords: Database-Assisted Design (DAD); Mean Recurrence Interval; Reinforced Concrete; Time-Domain Analysis; Point-In-Time Approach; Wind Effects.

Introduction

One of the problems encountered in the estimation of wind effects on high-rise structures is the development of combinations of wind-induced translational responses in possible conjunction with rotational responses. In addition, the design of structural members requires the estimation of combined effects consisting of demand-to-capacity ratios associated with (1) the axial force and bending moments and/or (2) shear forces and the torsional moment, in typical interaction equations.

Current wind engineering practice is based largely on frequency domain techniques, which in practice entail the loss of phase information. If the frequency domain approach is used, peaks can be calculated by a variety of methods (see, e.g., Gurley et al. 1997). Although the spectral densities and cross-spectra of various types of responses (e.g., axial force due to one modal translational response and axial force due to a second modal translational response) can be estimated individually, the estimation of the combination of those responses is not currently performed in accordance with physically rigorous models, but rather, in large part, intuitively, meaning that large numbers—as many as tens—of wind effect combinations are posited, which are assumed to result in reasonably safe designs. In current wind engineering practice it is common to use the empirical point-in-time (PIT) procedure for the estimation of peaks of combined stationary stochastic processes [see, e.g., references in Skidmore, Owings, and Merrill LLP (SOM) 2004]. The procedure is applied to pairs of such processes, and consists of adding an estimate of the peak value of one of the processes to the estimated value of the second process at the time of the occurrence of that peak. Some wind engineering laboratories that employ frequency domain approaches use the following oversimplified version of the PIT approach for estimating, for example, the 720-year combination of the effects resulting from (1) sway along one of the principal axes of the building and (2) sway along the second principal axis. First, estimate the 720-year value of the sway along one of the principal axes. Second, estimate the value of the 50-year sway along the other axis (the tacit, arbitrary assumption being that this value is equal to the PIT value corresponding to the 720-year peak). Finally, add these two estimates (for details see, e.g., references in SOM 2004). Even if a more accurate version of the PIT procedure were used, in which the full time histories of the two stochastic processes of interest were used, errors inherent in that procedure can be as high as 20%, as will be shown subsequently in this paper.

In recent years, time-domain techniques for estimating wind effects have been developed as the result of progress in pressure measurement technology and the availability of increasingly powerful computing capabilities. Time-domain techniques preserve phase relationships among all of the effects that come into play in structural design. In particular, the approach known as database-assisted design (DAD) allows for the calculation of a time series of combined wind effects that determine the structural design of individual members and for the assessment of the compliance of the

[1]IPA Research Engineer, National Institute of Standards and Technology, Gaithersburg, MD 20899. E-mail: donghun.yeo@nist.gov

Note. This manuscript was submitted on February 21, 2011; approved on May 16, 2012; published online on May 18, 2012. Discussion period open until August 1, 2013; separate discussions must be submitted for individual papers. This paper is part of the ***Journal of Structural Engineering***, Vol. 139, No. 3, March 1, 2013. ©ASCE, ISSN 0733-9445/2013/3-462–471/$25.00.

J. Struct. Eng. 2013.139:462-471.

structure with serviceability criteria. The DAD approach is applicable to both rigid and flexible buildings and has been introduced in Chapter C31 of ASCE 7-10 (ASCE 2010).

Calculations in DAD differ from simultaneous pressure integration, which is largely limited to providing information on wind loading. Rather, DAD focuses on estimating wind effects used in design and in checking the adequacy of the performance of individual members and of the structure as a whole. Individual internal forces and moments present in design interaction equations (i.e., axial force, bending moments, shear forces, and torsional moment), caused by the response in any number of modes, are obtained automatically by simple mathematical formulas (typically vectorial addition), regardless of whether the structures have coincident or noncoincident elastic and mass centers. This is also true of accelerations.

The purpose of this study is to present a multiple points-in-time (MPIT) approach to the efficient and accurate estimation of peaks of time series representing combinations of wind effects considered in design. For specificity, the MPIT approach is presented for the particular case of flexible reinforced concrete buildings, for which a DAD procedure has been developed by Yeo (2010) and Yeo and Simiu (2011). However, the approach is similar for other types of buildings, including rigid buildings or flexible steel buildings.

Multiple Points-in-Time Approach

In engineering practice it is necessary to estimate the peak of combinations of two or more individual effects. Several approaches have been developed using deterministic or probabilistic procedures. These include the PIT approach [sometimes referred to as Turkstra's rule (Turkstra 1970; Turkstra and Madsen 1980), the Ferry-Borges model (Ferry-Borges and Castanheta 1971), and Wen's model (Wen 1977)]. Whereas a version of the PIT approach has been used in wind engineering practice, as was noted earlier, to our knowledge, the Ferry-Borges and Wen models have not found application to the combination of stochastic processes induced by the same wind storm. This work develops and applies the MPIT approach to obtain accurately the desired peak combined effect. MPIT may be viewed as a more elaborate version of the empirical PIT approach, and it yields far more accurate results than PIT.

To fix the ideas, we consider the following example. The combined effect being considered is $X(t) = X_1(t) + X_2(t) + X_3(t)$, where $X_1(t)$, $X_2(t)$, and $X_3(t)$ = time histories of individual effects, and t = time. Each effect has 200 time steps. We select, for each time series, the n first largest peaks. For example, $n = 1, 3, 5,$ or 10. We consider all four of these values of n to investigate the effect of n on the accuracy of the approach. Fig. 1 shows time histories of $X_1(t)$, $X_2(t)$, $X_3(t)$, and $X(t)$, where the estimated highest peaks of individual and combined effects are identified by circles. For $n = 3$, the combined effects are estimated from a total of three time histories times $n = 3$ peaks per time history, that is, from a total of nine individual peaks. The estimated peak of the combined wind effects is the largest of the nine values consisting of the nine combined effects $X(t_i)$ $(i = 1, 2, \ldots, 9)$. The estimated peaks are 9.25 for $n = 1$, and 10.57 for all values $2 \le n \le 200$. This shows that, in this case, the MPIT approach estimates reliably and efficiently the peak of combined effect using $n = 2$ peaks per time series, instead of the full time series (FT) ($n = 200$). The combined effect in this example consists of a linear combination of time series; however, linearity is not required in this approach, as will be shown subsequently.

Combined Wind Effects Considered in Design

The DAD procedure for the design of high-rise reinforced concrete buildings accounts for combined wind effects on the structure using

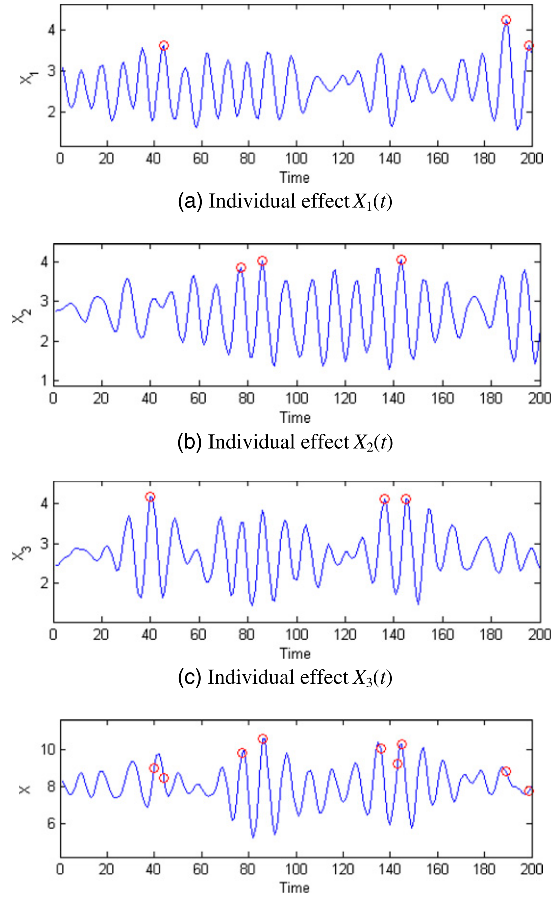

(a) Individual effect $X_1(t)$

(b) Individual effect $X_2(t)$

(c) Individual effect $X_3(t)$

(d) Combined effect $X(t)$ ($= X_1(t) + X_2(t) + X_3(t)$)

Fig. 1. Example of MPIT approach: (a) $X_1(t)$, (b) $X_2(t)$, and (c) $X_3(t)$ for individual effect; (d) $X(t)$ for combined effect

two types of response: (1) accelerations at the top floor and (2) demand-to-capacity indexes (DCIs) of member cross sections.

Top-Floor Acceleration

The time series of the resultant acceleration at the top floor, $a_{\text{top}}(t)$ is yielded by the expression

$$a_{\text{top}}(t) = \sqrt{\left[\ddot{x}_{\text{top}}(t) - D_{\text{top},y}\,\ddot{\theta}_{\text{top}}(t)\right]^2 + \left[\ddot{y}_{\text{top}}(t) + D_{\text{top},x}\,\ddot{\theta}_{\text{top}}(t)\right]^2} \quad (1)$$

where accelerations $\ddot{x}_{\text{top}}(t)$, $\ddot{y}_{\text{top}}(t)$, and $\ddot{\theta}_{\text{top}}(t)$ of the mass center at the top floor = x, y, and θ (i.e., rotational) axes, and $D_{\text{top},x}$ and $D_{\text{top},y}$ = distances along x and y axes from the mass center to the point of interest on the top floor.

The resultant value of Eq. (1) is used, rather than accelerations along the principal axes, because it is the peak acceleration, regardless of its direction, that is of concern for human discomfort. While ASCE 7-10 does not provide wind-related peak acceleration limits, for office buildings a limit of 25 mg with a 10-year mean recurrence interval (MRI) was suggested by Isyumov et al. (1992) and Kareem et al. (1999) (mg denotes milli-g, where g is the gravitational acceleration).

J. Struct. Eng. 2013.139:462-471.

Demand-to-Capacity Indexes

A DCI is a quantity used to measure the adequacy of the strength of a structural member. For a member cross section, the DCI is defined as a function of the internal forces and/or moments induced by the design loads, each divided by the corresponding capacity of the cross section. The capacity is based on ACI 318-08 [American Concrete Institute (ACI) 2008]. An index higher than unity indicates inadequate design; the index must be less than or equal to unity for the design to be acceptable. DAD has two DCIs: (1) for axial and/or flexural loads and (2) for shear and torsional loads.

For cross sections subjected to axial force and bending moments, the DCI is denoted by B_{ij}^{PM} [as in Yeo (2010); subscript i = member i and subscript j = cross section j of that member]. In the case of beams and columns whose sections are subjected to a bending moment and an axial force, the DCI has the simple expressions:

$$B_{ij}^{PM}(t) = \frac{M_u(t)}{\phi_m M_n} \qquad \text{(for tension-controlled sections)} \tag{2a}$$

$$B_{ij}^{PM}(t) = \frac{P_u(t)}{\phi_p P_n} \qquad \text{(for compression-controlled sections)} \tag{2b}$$

where $M_u(t)$ and $P_u(t)$ = design bending moment and design axial force at the cross section being considered, M_n and P_n = nominal bending moment and axial force capacities of the cross section, and ϕ_m and ϕ_p = reduction factors for flexural and axial strength, respectively. M_n and P_n depend upon the location of P_u and M_u in the axial load-bending moment interaction diagram (the PM diagram) of the column section, as specified in code ACI 318-08. For beams with no axial force, the DCI is calculated by using Eq. (2a) for tension-controlled sections.

For columns subject to biaxial flexure loads, the PCA load contour method [Portland Cement Association (PCA) 2008] is used for tension-controlled sections:

$$\begin{aligned} B_{ij}^{PM}(t) &= \frac{M_{ux}(t)}{\phi_m M_{nox}}\left(\frac{1-\beta}{\beta}\right) + \frac{M_{uy}(t)}{\phi_m M_{noy}} \qquad \text{for} \quad \frac{M_{uy}(t)}{M_{ux}(t)} > \frac{M_{noy}}{M_{nox}} \\ B_{ij}^{PM}(t) &= \frac{M_{ux}(t)}{\phi_m M_{nox}} + \frac{M_{uy}(t)}{\phi_m M_{noy}}\left(\frac{1-\beta}{\beta}\right) \qquad \text{for} \quad \frac{M_{uy}(t)}{M_{ux}(t)} < \frac{M_{noy}}{M_{nox}} \end{aligned} \tag{3}$$

where $M_{ux}(t)$ = design bending moment about x axis, $M_{uy}(t)$ = design bending moment about y axis, M_{nox} = nominal uniaxial moment strength about x axis, M_{noy} = nominal uniaxial moment strength about y axis, and β = constant dependent upon the properties and details of the member, for which the value 0.65 is typically used as an approximation. Note that the x and y axes are the principal axes of the cross section under consideration.

For compression-controlled sections, the Bresler reciprocal load method [ACI 318-08 (R10.3.6)] is used:

$$B_{ij}^{PM}(t) = \frac{P_u(t)}{\phi_p P_n} = \frac{P_u(t)}{\phi_p \dfrac{1}{\dfrac{1}{P_{ox}} + \dfrac{1}{P_{oy}} - \dfrac{1}{P_o}}} \tag{4}$$

where P_{ox} = maximum uniaxial load strength of column with moment $M_{nx} = P_n e_y$ (e_y = eccentricity along y axis), P_{oy} = maximum uniaxial load strength of column with moment $M_{ny} = P_n e_x$ (e_x = eccentricity along x-axis), and P_o = maximum axial load strength with no applied moments.

For cross sections subjected to shear forces and torsional moment, the DCI is denoted by B_{ij}^{VT}:

$$B_{ij}^{VT}(t) = \frac{\sqrt{V_u^2(t) + \left[\dfrac{T_u(t) p_h\, b_w d}{1.7 A_{oh}^2}\right]^2}}{\phi_v (V_c + V_s)} \tag{5}$$

where V_c and V_s = nominal shear strengths provided by concrete and by reinforcement, respectively, $V_u(t)$ = shear force, $T_u(t)$ = torsional moment, ϕ_v = reduction factors for shear strengths, p_h = perimeter enclosed by the centerline of the outermost closed stirrups, A_{oh} = area enclosed by centerline of outermost closed stirrups, b_w = width of member, and d = distance from extreme compression fiber to the centroid of longitudinal tension reinforcement. Note that the concrete shear strength V_c varies depending on the axial force acting on the cross section.

For members subject to biaxial shear forces, the DCI is

$$B_{ij}^{VT}(t) = \frac{\sqrt{V_{ux}^2(t) + V_{uy}^2(t) + \left[\dfrac{T_u(t) p_h\, b_w d}{1.7 A_{oh}^2}\right]^2}}{\phi_v (V_c + V_s)} \tag{6}$$

where V_{ux} and V_{uy} = shear forces along x and y axes, respectively.

Application of MPIT Approach to Wind Effects

Peaks of combined wind effects (i.e., the resultant top-floor acceleration and DCIs) are obtained from their full time histories for all wind speeds (e.g., 20 m/s, 30m/s,. . ., 80 m/s) and all wind directions (e.g., 0°, 10°,. . ., 350°) of interest, and are used to produce response databases (or wind effect databases) that consist of wind effects as functions of wind speed and direction. Construction of response databases from an FT of wind effects requires considerable computational time. In particular, this is the case when calculating the DCIs for thousands of structural members in high-rise buildings, and even more so when two DCIs are used as a measure of member adequacy in strength design.

Let the number of peaks used for the MPIT approach be n. To estimate peak top-floor accelerations (caused by the resultant of translational and rotational motions along both principal directions) and peak DCIs (resulting from internal forces and moments), the application of the MPIT approach is similar to the approach illustrated in the Multiple Points-in-Time Approach section (see Appendix for details).

For an example of the MPIT approach as applied to DCIs, consider the estimation of the peak combined effect denoted by B_{ij}^{PM} of a column for a specified wind speed and direction. Set the number of peak values for each time history of individual effects (P_u, M_{ux}, and M_{uy}) to be $n = 5$. Ten peaks (i.e., the five highest peaks and the five lowest peaks) are chosen from the time series of P_u, five peaks are chosen from the time history of M_{ux}, and five peaks are chosen from the time history of M_{uy}, as shown in Fig. 2, where the peaks are depicted as circles. Thus, the total number of times, denoted by $n*$, required to calculate the DCI is $4 \times 5 = 20$. However, some of those times coincide, so $n* = 16$ in this example. The MPIT approach estimates 16 DCI values, whereas an FT approach would entail the calculation of 7,305 DCI values per member (i.e., one value for each of the ordinates of the time series in this example). The DCI plot

J. Struct. Eng. 2013.139:462-471.

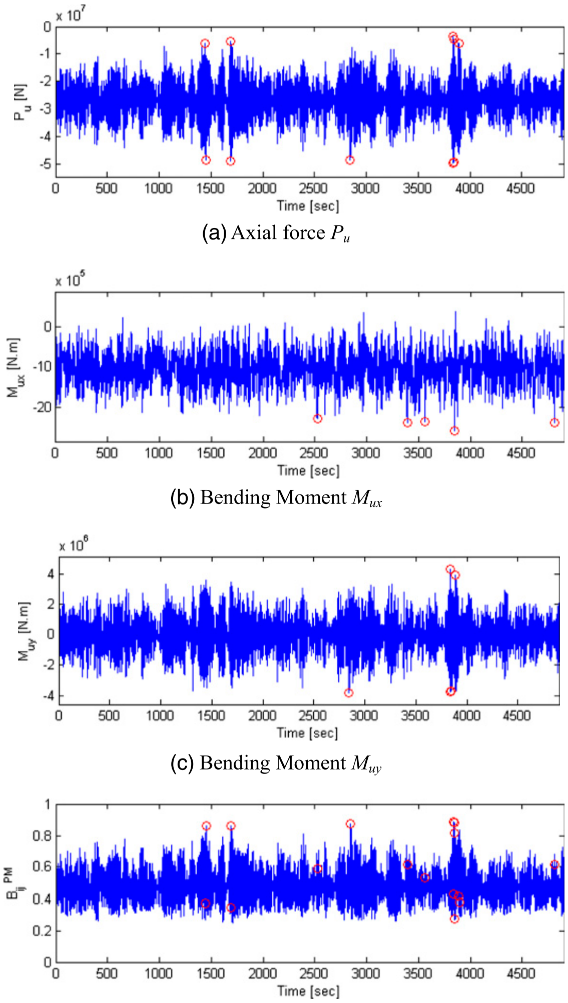

(a) Axial force P_u

(b) Bending Moment M_{ux}

(c) Bending Moment M_{uy}

(d) DCI

Fig. 2. Peaks in time histories: (a) P_u; (b) M_{ux}; (c) M_{uy}; (d) DCI

[Fig. 2(d)] shows that the estimated peak of MPIT is identical to the observed peak of the FT approach. This is an indication that the MPIT approach results in reliable estimates of the highest peak of the combined wind effect.

The advantage of MPIT is its significantly reduced calculation time. An effective MPIT approach requires the selection of a number n, which should be sufficiently small enough for computational efficiency and sufficiently large enough to yield accurate results.

Application to a 60-Story CAARC Building

A high-rise reinforced concrete building was designed using the High-Rise Database-Assisted Design for Reinforced Concrete structures [*HR_DAD_RC* NIST 2010)] software and the MPIT approach. The MPIT approach was based on the following numbers, *n,* of peaks: $n = 1, 3, 5, 10, 12$ and 40, for each internal force, moment, and acceleration. The optimal number n was determined by comparing the results of the calculations. In addition, the FT approach was also employed for comparison.

The design building was assumed to be a 60-story reinforced concrete building with rigid diaphragm floors (Fig. 3) and is known as the Commonwealth Advisory Aeronautical Research Council (CAARC) building (Melbourne 1980; Venanzi 2005; Wardlaw and Moss 1971). Its dimensions are 45.72 m in width (B in Fig. 3), 30.48 m in depth (D), and 182.88 m in height (H). The building has a moment-resisting frame structural system, similar to the structural system with comparable dimensions studied by Teshigawara (2001), and consists of 7,800 members (i.e., 2,880 columns and 4,920 beams). The building was assumed to be located in suburban terrain exposure near Miami.

Modeling of the Building

Structural members of the building consist of columns, beams, and slabs. Columns are divided into corner and noncorner columns, and beams are divided into exterior (spandrel) and interior beams. As shown in Table 1, the building is composed of six sets of members. Each set consists of 10 stories in which the member dimensions and reinforcement details are the same. The first set applies to the first 10 stories, the second to the next 10 stories, and so forth. The compressive strengths of concrete for all members are 80 MPa from the first to the 40th stories and 60 MPa from the 41st to the 60th stories. Columns have longitudinal reinforcement uniformly distributed along the sides and hoops, and beams have tensile and compression reinforcement and stirrups. The yield strengths of reinforcements are 520 MPa for longitudinal bars and 420 MPa for hoop or stirrup bars. Wind effects were calculated for a typical set of 96 members (Fig. 4) out of 7,800 beams and columns, and slabs were not designed in this study.

For dynamic properties of the design building, natural frequencies of vibration considered in this study are 0.165 Hz for the first mode in the y direction, 0.175 Hz for the second mode in the x direction, and 0.200 Hz for the θ direction (Fig. 5). The corresponding modal damping ratios were assumed to be 2% in all three modes.

Response Databases from Aerodynamic Pressure Data

For wind with speeds of 20 m/s to 80 m/s in increments of 10 m/s and wind directions of 0° to 350° in increments of 10°, dynamic analyses were performed using time histories of aerodynamic wind loads at the mass center of each floor, calculated from time series of aerodynamic pressures on a rigid model of the CAARC building measured in wind tunnel tests (Venanzi 2005). The analyses yielded time series of motion and effective lateral loads at the mass centers. The motion time series yielded values of the top floor acceleration. The lateral loads caused by wind, multiplied by influence coefficients, yielded internal forces and moments at critical sections of members. The combination of these internal forces and moments with internal forces and moments caused by gravity loads specified by ASCE 7-10, Section 2.3, yielded combined DCIs at the critical cross sections. This study accounts for one load combination case for serviceability design [LC in Eq. (7a)], and two cases for strength design [LC1 and LC2 in Eq. (7b)]:

$$1.0D + 1.0L + 1.0W \qquad \text{(LC)} \tag{7a}$$

$$\begin{aligned} &1.2D + 1.0L + 1.0W \qquad \text{(LC1)} \\ &0.9D + 1.0W \qquad \text{(LC2)} \end{aligned} \tag{7b}$$

where D = total dead load, L = live load, and W = wind load.

Response databases for the resultant acceleration and DCIs were constructed using their peak values for each wind direction and each wind speed. Thus, once a wind direction and a wind speed are specified, the associated combined wind effects can be obtained using the response databases. The construction of response databases

J. Struct. Eng. 2013.139:462-471.

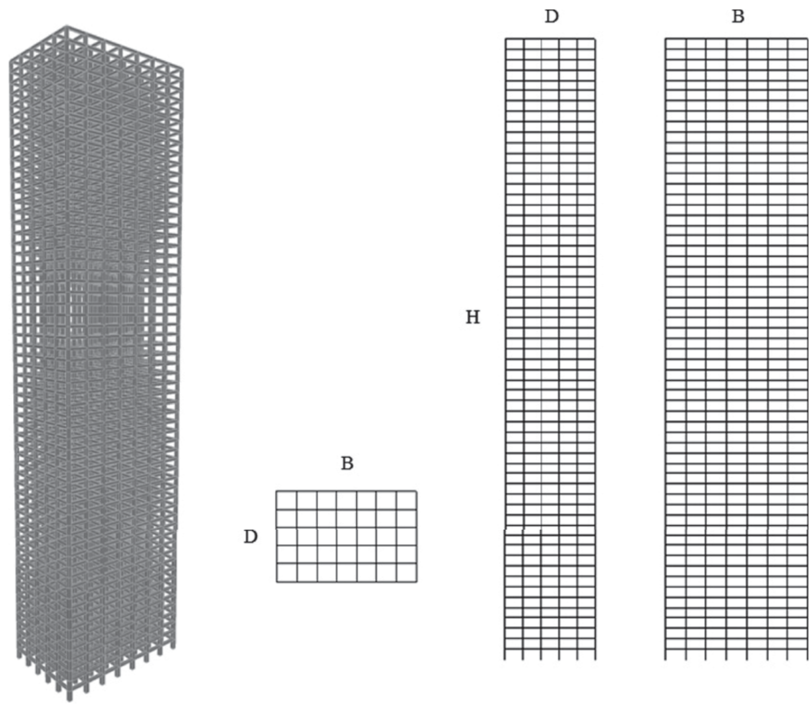

Fig. 3. Schematic views of 60-story building

Table 1. Section Dimensions and Reinforcement Details for Critical Sections of Structural Members

Name	Story	Section [mm × mm]	Longitudinal bar	Hoop or stirrup [spacing: mm]	Selected member
Corner column (cc)	51 ~ 60	750 × 750	12 − D29	4 − D13@200	6, 12, 18, 24 (51st story)
	41 ~ 50	750 × 750	12 − D29	4 − D13@200	5, 11, 17, 23 (41st story)
	31 ~ 40	800 × 800	16 − D32	4 − D13@200	4, 10, 16, 22 (31st story)
	21 ~ 30	850 × 850	20 − D32	4 − D16@200	3, 9, 15, 21 (21st story)
	11 ~ 20	900 × 900	20 + 12 − D43	4 − D16@200	2, 8, 14, 20 (11th story)
	1 ~ 10	1100 × 1100	24 + 16 − D43	4 − D16@200	1, 7, 13, 19 (1st story)
Noncorner column (cn)	51 ~ 60	750 × 750	12 − D25	4 − D13@200	6, 12, 18, 24 (51st story)
	41 ~ 50	750 × 750	12 − D25	4 − D13@200	5, 11, 17, 23 (41st story)
	31 ~ 40	800 × 800	12 − D25	4 − D16@200	4, 10, 16, 22 (31st story)
	21 ~ 30	850 × 850	16 − D29	4 − D16@200	3, 9, 15, 21 (21st story)
	11 ~ 20	900 × 900	20 + 12 − D43	4 − D16@200	2, 8, 14, 20 (11th story)
	1 ~ 10	1100 × 1100	20 + 16 − D43	4 − D16@200	1, 7, 13, 19 (1st story)
Exterior beam (be)	51 ~ 60	400 × 700	4 − D32 / 2 − D32	2 − D13@150	6, 12, 18, 24 (roof)
	41 ~ 50	400 × 700	4 + 4 − D32 / 3 − D32	2 − D16@150	5, 11, 17, 23 (50th floor)
	31 ~ 40	450 × 750	4 + 4 − D36 / 4 − D32	4 − D16@150	4, 10, 16, 22 (40th floor)
	21 ~ 30	500 × 750	5 + 5 − D36 / 4 − D36	4 − D16@150	3, 9, 15, 21 (30th floor)
	11 ~ 20	550 × 750	5 + 5 − D43 / 4 − D36	4 − D16@150	2, 8, 14, 20 (20th floor)
	1 ~ 10	550 × 800	5 + 5 − D43 / 4 − D36	4 − D16@150	1, 7, 13, 19 (10th floor)
Interior beam (bi)	51 ~ 60	400 × 700	4 − D29 / 2 − D29	2 − D13@150	6, 12, 18, 24 (roof)
	41 ~ 50	400 × 700	4 + 4 − D32 / 2 − D32	2 − D13@150	5, 11, 17, 23 (50th floor)
	31 ~ 40	450 × 750	4 + 4 − D36 / 3 − D32	4 − D13@150	4, 10, 16, 22 (40th floor)
	21 ~ 30	500 × 750	5 + 5 − D36 / 4 − D36	4 − D13@150	3, 9, 15, 21 (30th floor)
	11 ~ 20	550 × 750	5 + 5 − D36 / 4 − D36	4 − D13@150	2, 8, 14, 20 (20th floor)
	1 ~ 10	550 × 800	5 + 5 − D36 / 4 − D36	4 − D13@150	1, 7, 13, 19 (10th floor)

Note: cc1 ~ cc24 for corner columns; cn1 ~ cn24 for noncorner columns; be1 ~ be24 for exterior beams; bi1 ~ bi24 for interior beams.

requires a considerable amount of computation, because hundreds of dynamic analyses need to be performed for the various wind directions and wind speeds. Whereas response databases of top-floor resultant accelerations are typically required for corners of the building on the floor, response databases of DCIs may be required for large numbers of members. This entails a large amount of computational time, which can be significantly reduced by the MPIT approach.

Fig. 6, in which θ_w denotes the wind direction, shows an example of response database of a DCI for a corner column (cc1) under load combination LC1. Note that the response database for any wind

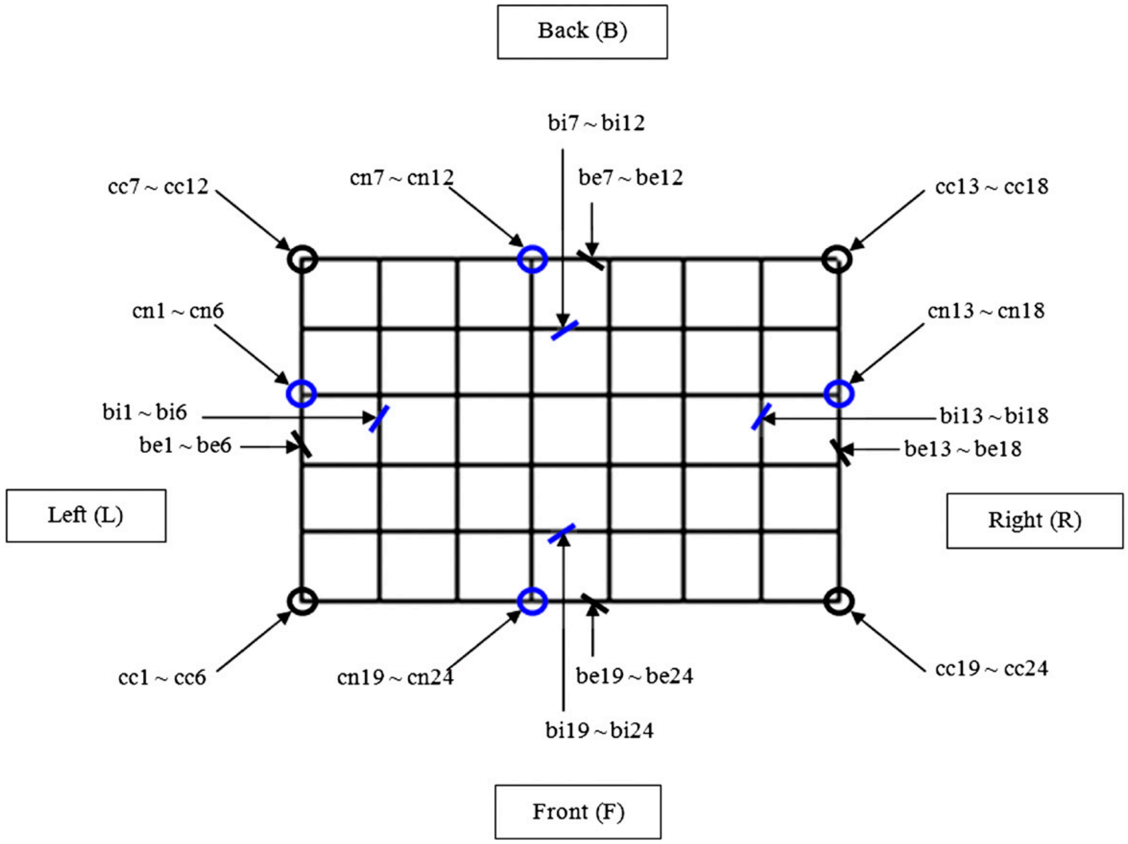

Fig. 4. Plan view of building with locations of selected members ($\alpha = 0°$): cc, corner column; cn, noncorner column; be, exterior beam; bi, interior beam

speed and direction is a property of the structure, that is, it is independent of wind climate.

Structural Responses Induced by Wind Climate

Structural responses under the wind climate at a location near Miami were obtained by applying to the response databases the directional wind speeds from the climatological database at or near that location. The climatological database used in the study is a dataset of 999 simulated hurricanes with wind speeds for 16 directions near Miami (Milepost 1,450; available at www.nist.gov/wind). The left side of the building was assumed to face south (i.e., $\alpha = 0°$ in Fig. 5).

The terrain exposure near the building was assumed to be suburban (i.e., Exposure Category B) in all directions. The DAD procedure modified the climatological database of the directional wind speeds by basing it on hourly mean wind speeds (m/s) at the building rooftop in suburban terrain exposure (see Section 11.1.2 in Simiu 2011 and Section 26.9.5 in ASCE 7-10). The climatological database of directional wind speeds for the 999 extreme windstorms was applied to each response database. From the largest directional response for each of the 999 windstorms, the corresponding 999 largest responses, regardless of wind direction, were obtained. A nonparametric method for estimating peak responses corresponding to specified MRIs of the wind effects was then applied as in Section 12.7 of Simiu (2011).

Fig. 7 shows peak accelerations of the front-left (i.e., the southeast) corner of the top floor, and Fig. 8 shows peak DCIs of the corner column cc1 for LC1. These combined wind effects were estimated as functions of MRIs.

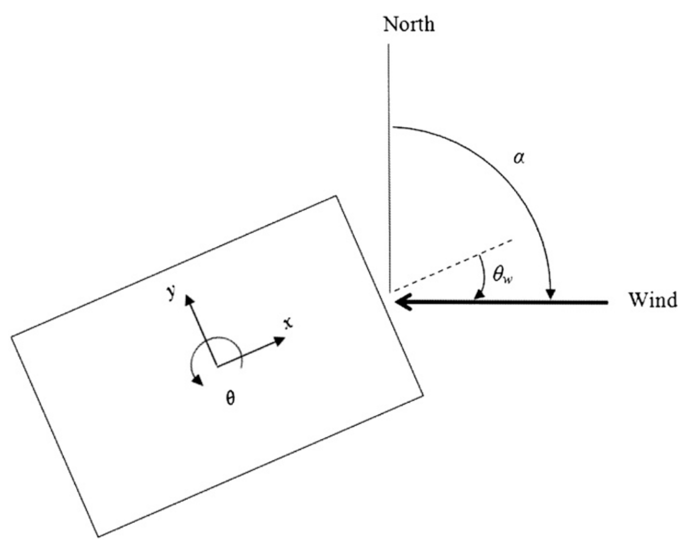

Fig. 5. Local coordinates of building and wind directions

Adjustment of Demand-to-Capacity Indexes

DAD accounts for the ASCE 7-10 requirement that overturning moments determined by wind tunnel testing must not be less than 80% of their ASCE 7-based counterparts (see ASCE 7-10, Section 31.4.3). ASCE 7-based overturning moments about the principal axes (i.e., x and y axes) of buildings with Risk Category III and IV

J. Struct. Eng. 2013.139:462-471.

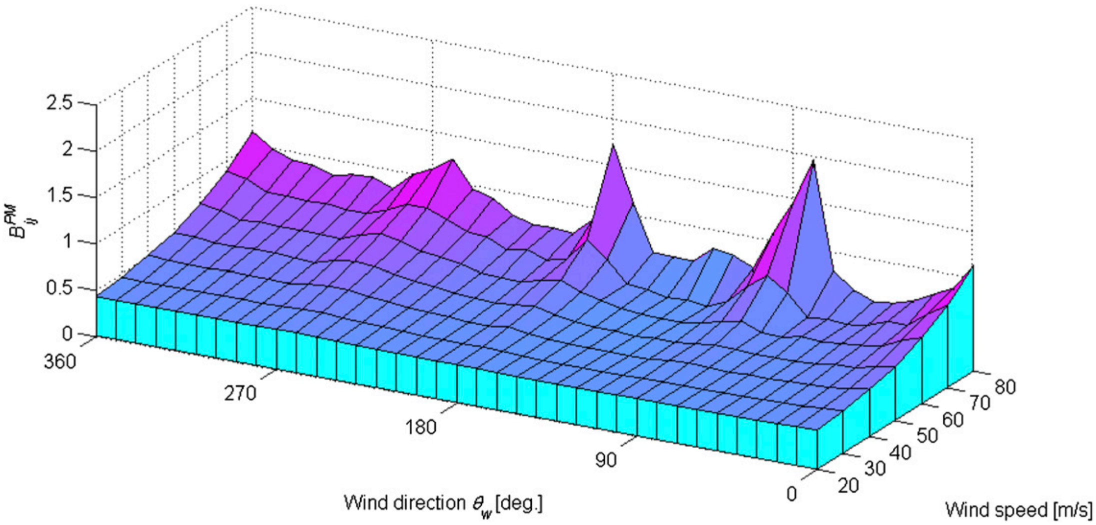

Fig. 6. Response database: DCI (member ID = cc1)

were therefore calculated for a basic wind speed of 81 m/s based on MRI = 1,700 years (Table C26.5-3 in ASCE 7-10) and were compared with the peak overturning moments determined by the DAD procedure for that MRI.

If the moments in DAD are less than 80% of those determined in accordance with Part I of Chapter 27 of ASCE 7-10, the DCIs were adjusted as follows:

$$B_{ij}^* = \gamma B_{ij}$$
$$\text{where } \gamma = \frac{0.8}{M_o^{\mathrm{DAD}}/M_o^{\mathrm{ASCE7}}} \tag{8}$$

where M_o^{DAD} and M_o^{ASCE7} = overturning moments at base obtained from DAD and Part I of Chapter 27, ASCE 7-10, respectively, and γ = index adjustment factor. If the moment in DAD is not less than 80% of the ASCE 7-10 value, the index need not be modified (i.e., $B_{ij}^* = B_{ij}$).

As shown in Table 2, ratios of overturning moments from DAD to those from ASCE 7 are less than 0.8 on the x axis, and the corresponding index adjustment factor γ [Eq. (8)] is 1.12. Adjusted DCIs for MRI = 1,700 years were obtained by multiplying the indexes by the adjustment factors.

MPIT-Based Wind Effects

This study applied PIT, MPIT, and FT approaches to calculating peak combined wind effects for appropriate MRIs (i.e., resultant acceleration for a 10-year MRI and adjusted DCIs for a 1,700-year MRI). Note that PIT is a particular case of the MPIT approach in which the number of peaks is $n = 1$. The top-floor accelerations of the southeast corner were calculated under the load combination case LC [Eq. (7a)], and the DCIs of 96 selected members were estimated under the load combination cases LC1 and LC2 [Eq. (7b)]. The DCIs being considered are the higher of the values obtained for these load combinations. The DCIs described subsequently are adjusted DCIs.

Fig. 9 shows typical examples of the combined wind effects estimated by these approaches. As n increases, the estimated peak value of resultant acceleration and DCIs based on MPIT rapidly converges to the observed peak value of their full series in FT. This indicates that the MPIT approach estimates peak DCIs more effectively than the PIT approach. Table 3 compares the performance

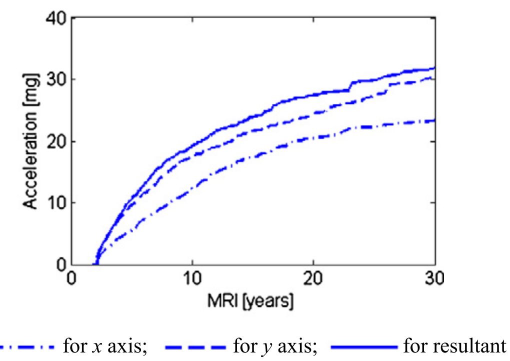

Fig. 7. Peak top-floor accelerations

of the three approaches. For the resultant acceleration, R_a denotes the ratio of PIT- or MPIT-based values to the FT-based value. For DCIs, N_m denotes the number of members out of 96 members whose DCIs based on MPIT are not identical to the values based on FT, and R_m denotes the lowest ratio of MPIT-based DCI to FT-based DCI. The MPIT approach calculated the acceleration and DCIs for at most $3n$ and $4n$ local peak points, respectively (e.g., for $n = 10$, 30 points for acceleration and 40 points for DCIs). In contrast, the FT approach used 7,305 points of the full time history. As shown by the results of the calculations, the PIT approach shows an ~10% error in the estimated acceleration and 10–20% errors in the estimated DCIs. The MPIT approach, however, significantly improves the performance of their estimation; the acceleration and DCIs estimated from MPIT using $n \geq 10$ are at least 98% of those calculated from FT.

Fig. 10 describes the computational time of the PIT and MPIT approaches relative to that of the FT approach. PIT took less than 10% of the computational time of FT, and the computational time of MPIT increased almost negligibly as n increased; the MPIT approach using $n = 40$ increases the time by only 2% in comparison with the time required for the PIT approach. These results show that the MPIT approach is more efficient than the FT approach and is more reliable than the PIT approach, for both linear and nonlinear combinations of individual wind effects.

For design wind effects estimated by the MPIT approach using $n = 10$, the estimated peak top floor resultant acceleration is 18.3 mg

J. Struct. Eng. 2013.139:462-471.

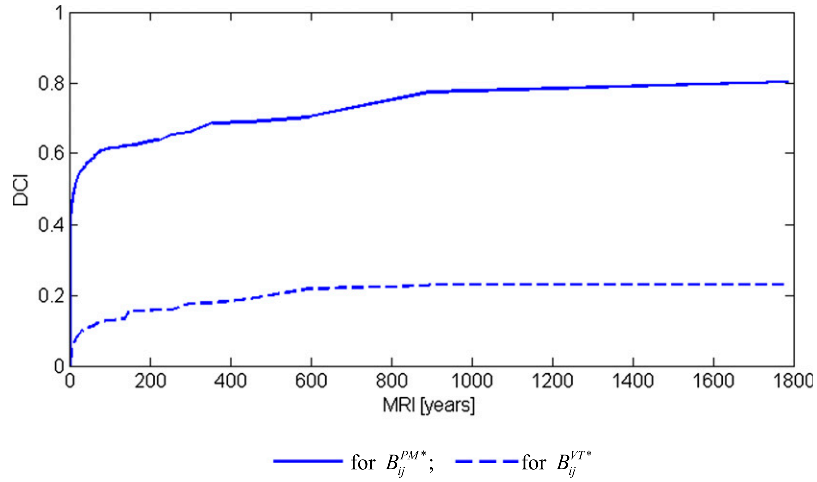

Fig. 8. Peak DCIs

Table 2. Overturning Moments and Adjustment Factor

Method	$M_{ox}[\times 10^6 \text{ kN}\cdot\text{m}]$	$M_{oy}[\times 10^6 \text{ kN}\cdot\text{m}]$	$M_{ox}^{\text{DAD}}/M_{ox}^{\text{ASCE7}}$	$M_{oy}^{\text{DAD}}/M_{oy}^{\text{ASCE7}}$	γ
ASCE 7-10	6.49	3.92	0.72	0.97	1.12
DAD	4.64	3.81			

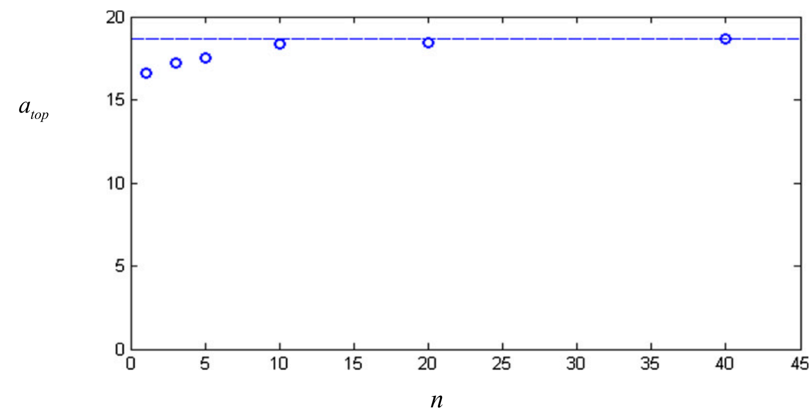

(a) Top-floor resultant acceleration
(circle for PIT (n = 1) and MPIT (n = 3 – 40); dotted line for FT)

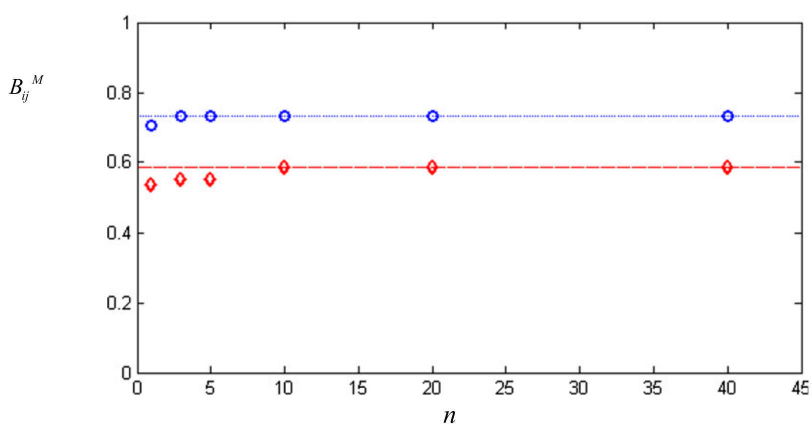

(b) DCIs
(For LC1, circle for PIT (n = 1) and MPIT (n = 3 – 40), dotted line for FT;
for LC2, diamond for PIT (n = 1) and MPIT (n = 3 – 40), solid line for FT)

Fig. 9. Estimation of wind effects from PIT, MPIT, and FT: (a) Top-floor resultant acceleration; (b) DCIs

J. Struct. Eng. 2013.139:462-471.

Table 3. Comparison of peak combined wind effects

Peak wind effect	Ratio	n = 1	3	5	10	20	40
a_{top}	R_a	0.89	0.92	0.94	0.98	0.99	1.00
B_{ij}^{PM*}	N_m (out of 96)	14	5	5	2	1	1
	R_m	0.91	0.98	0.98	0.99	0.99	0.99
B_{ij}^{VT*}	N_m (out of 96)	30	7	3	3	3	3
	R_m	0.83	0.99	0.99	0.99	0.99	0.99

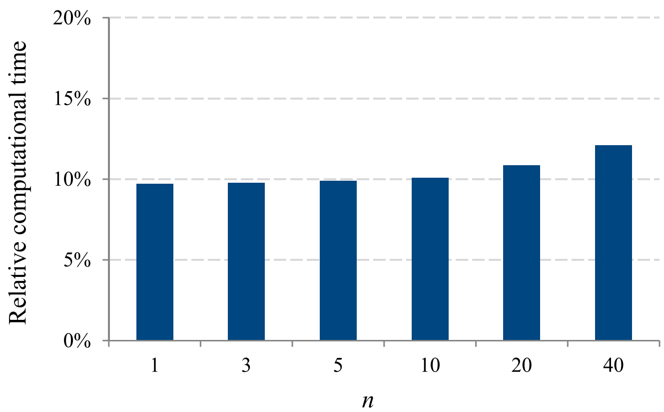

Fig. 10. Comparison of computational time

Table 4. Adjusted Peak DCIs

DCI	Corner column	Noncorner column	Exterior beam	Interior beam
B_{ij}^{PM*}	0.98	0.99	0.63	0.73
B_{ij}^{VT*}	0.64	0.50	0.53	0.70

for MRI = 10 years, that is, less than the 25 mg limit suggested by Isyumov et al. (1992). The design is, therefore, adequate for peak acceleration. The largest MPIT-based DCIs using $n = 10$ for the 96 members considered in this study are summarized in Table 4. The highest B_{ij}^{PM*} is 0.99 and the highest B_{ij}^{VT*} is 0.70, meaning that structural members were adequately designed for strength. That is, all members have the capacity to resist effects of interacting axial force and bending moments as well as effects of interacting shear forces and torsional moment corresponding to MRI of 1,700 years.

The results show that the MPIT procedure using $n = 10$ peak points is both economical in terms of computational time as well as being remarkably accurate for estimating peak combined wind effects. Note that one of the advantages of our time-domain approach is that it does not require the development and use of many unwieldy, unavoidably error-prone load combinations based on guesswork rather than on analysis.

Conclusions

A methodology using the MPIT approach was developed in this study to achieve the reliable and efficient estimation of peak combined wind effects. The accuracy of the MPIT approach was found to be superior to the accuracy of the PIT approach, and to be close to the accuracy of calculations based on the FT of the processes being combined. Its computer time requirements are of the same order as for PIT, and significantly reduced with respect to those for FT.

The validity of the MPIT approach was investigated for a 60-story reinforced concrete building. To obtain peak combined wind effects of (1) top-floor resultant acceleration and (2) demand-to-capacity indexes (DCIs), various numbers n of peaks of the individual time series (i.e., $n = 1, 3, 5, 10, 20$ and 40) were used, and the respective peak combined wind effects were calculated at the points in time corresponding to those peaks. The largest of those combined wind effects was selected as the peak combined wind effect being sought. The MPIT-based DCIs were compared with peaks of the full time series, that is, with the peak DCIs for all data points in the time history. The comparisons showed that the MPIT approach based on $n = 10$ yielded reliable peak combined wind effects, whereas the computational time was reduced to ∼10% of the times required for the FT approach. This is viewed as a useful verification of the validity of the MPIT approach.

Like PIT, MPIT is an empirical procedure. The development of the PIT approach proceeded in two phases. The first phase consisted of the presentation and verification of the approach (Turkstra 1970). A second phase consisted of an effort to provide theoretical justification for PIT (Madsen 1997). A similar sequence is envisaged for MPIT; the author is planning to develop its theoretical foundations, and others may join in this effort.

By construction, the performance of MPIT is indisputably superior to the performance of PIT. This has been confirmed by the results obtained in this investigation. The MPIT-based DAD developed in this study provided accurate combined wind effects not obtainable by the frequency domain approach, and significantly reduced the amount of computational time of a conventional time domain analysis required by a full time-histories approach.

Appendix

Choice of Peaks in Individual Time Series

The MPIT procedure makes use of rank-ordered peaks in each time history of individual effects (e.g., internal forces and moments, and accelerations caused by motions along the two principal horizontal directions and by torsional motion). For the calculation of the resultant acceleration, n highest peaks are selected for the absolute values of the time series of $\ddot{x}_{\text{top}}$, $\ddot{y}_{\text{top}}$, and $\ddot{\theta}_{\text{top}}$; for the calculation of B_{ij}^{PM} (pertaining to interaction of axial force P_u and bending moments M_{ux} and M_{uy} in the x and y principal axes), n highest negative peaks and n highest positive peaks are selected for the time series of P_u, and n highest peaks are selected from the absolute values of the time histories of M_{ux} and M_{uy}. The n negative peak values of P_u are associated with maximum compression for compression-controlled sections, and the n highest peak values are associated with maximum tension or minimum compression for tension-controlled sections (for details, see Eq. 2). (Negative values of P_u indicate compression.) For the calculation of B_{ij}^{VT} (pertaining to the interaction of the shear forces V_{ux} and V_{uy} and the torsional moment T_u), n highest peaks are selected from the absolute values of the time histories of V_{ux}, V_{uy}, and T_u. Additional n highest-peak values of P_u are used, because the shear strength of a section is reduced by the tensile axial force (see Section 11.2 in ACI 318-08). Thus, in general, there will be a total of $3n$ and $4n$ peak values to consider for the resultant acceleration and each DCI, respectively; for example, to establish a DCI response database in this case, $4n$ peak values are used for each wind direction and speed being considered. However, because the peak values can occur simultaneously (e.g., peaks of

J. Struct. Eng. 2013.139:462-471.

axial force and bending moment occur at the same time), in general, less than $4n$ are actually needed.

Acknowledgments

The author would like to thank Dr. Emil Simiu for valuable advice and comments. The wind tunnel data developed at the CRIACIV-DIC Boundary Layer Wind Tunnel, Prato, Italy, were kindly provided by Dr. Ilaria Venanzi of the University of Perugia.

References

American Concrete Institute (ACI). (2008). "Building code requirements for structural concrete and commentary." *ACI 318-08*, Farmington Hills, MI.

ASCE. (2010). "Minimum design loads for buildings and other structures." *ASCE 7-10*, Reston, VA.

Ferry-Borges, J., and Castanheta, M. (1971). *Structural safety*, 2nd Ed., National Civil Engineering Laboratory, Lisbon, Portugal.

Gurley, K. R., Tognarelli, M. A., and Kareem, A. (1997). "Analysis and simulation tools for wind engineering." *Probab. Eng. Mech.*, 12(1), 9–31.

Isyumov, N., Fediw, A. A., Colaco, J., and Banavalkar, P. V. (1992). "Performance of a tall building under wind action." *J. Wind Eng. Ind. Aerodyn.*, 42(1–3), 1053–1064.

Kareem, A., Kijewski, T., and Tamura, Y. (1999). "Mitigation of motions of tall buildings with specific examples of recent applications." *Wind Struct.*, 2(3), 201–251.

Madsen, H. O. (1997). "Stochastic modeling of load combinations." *Probabilistic methods for structural design*, C. G. Soares, ed., Springer, Netherlands, 227–243.

Melbourne, W. H. (1980). "Comparison of measurements on the CAARC standard tall building model in simulated model wind flows." *J. Wind Eng. Ind. Aerodyn.*, 6(1–2), 73–88.

NIST. (2010). "Database-assisted design software for high-rise buildings (*HR_DAD_RC ver. 1.0*)." ⟨http://www.itl.nist.gov/div898/winds/HR_DAD_RC_1.0/hr_dad_rc_1.0.htm⟩ (Jan. 3, 2013).

Portland Cement Association (PCA). (2008). *PCA notes on 318-08 building code requirements for structural concrete with design applications*, M. E. Kamara, L. C. Novak, and B. G. Rabbat, eds. Portland Cement Association, Skokie, IL.

Simiu, E. (2011). *Design of buildings for wind: A guide for ASCE 7-10 standard users and designers of special structures*, 2nd ed., Wiley, Hoboken, NJ.

Skidmore, Owings, and Merrill LLP (SOM). (2004). "WTC wind load estimates, outside experts for baseline structural performance Appendix D." in NIST NCSTAR1-2, Baseline structural performance and aircraft impact damage analysis of the World Trade Center towers, submitted by Skidmore, Owings and Merrill LLP, Chicago, Illinois, April 13, 2004 (wtc.nist.gov), also reproduced as Appendix to NIST Technical Note 1655, "Toward a standard on the wind tunnel method" (2009) by E. Simiu, pp. A1–A7 (www.nist.gov/wind).

Teshigawara, M. (2001). "Structural design principles." Chapter 6, *Design of modern highrise reinforced concrete structures*, H. Aoyama, ed., Imperial College Press, London.

Turkstra, C. J. (1970). "Theory of structural safety." *Technical Rep., SM Study No. 2*, Solid Mechanics Division, Univ. of Waterloo, Ontario, Canada.

Turkstra, C. J., and Madsen, H. O. (1980). "Load combination in condified structural design." *J. Struct. Div.*, 106(12), 2527–2543.

Venanzi, I. (2005). "Analysis of the torsional response of wind-excited high-rise building." Ph.D. thesis, Univ. degli Studi di Perugia, Perugia, Italy.

Wardlaw, R. L., and Moss, G. F. (1971). "A standard tall building model for the comparison of simulated natural winds in wind tunnels." *3rd Int. Conf. on Wind Effects on Buildings and Structures*, Saikon, Tokyo, 1245–1250.

Wen, Y. K. (1977). "Statistical combination of extreme loads." *J. Struct. Div.*, 103(5), 1079–1093.

Yeo, D. (2010). "Database-assisted design for wind: Concepts, software, and example for of high-rise reinforced concrete structures." *NIST Technical Note 1665*, National Institute of Standards and Technology, Gaithersburg, MD.

Yeo, D., and Simiu, E. (2011). "High-rise reinforced concrete structures: Database-assisted design for wind." *J. Struct. Eng.*, 137(11), 1340–1349.